Bioresource Technology 255 (2018) 39–49

Contents lists available at ScienceDirect

Bioresource Technology

journal homepage: www.elsevier.com/locate/biortech

Life cycle, techno-economic and dynamic simulation assessment of bioelectrochemical systems: A case of formic acid synthesis

Mobolaji Shemfe[a], Siddharth Gadkari[b], Eileen Yu[c], Shahid Rasul[c], Keith Scott[c], Ian M. Head[d], Sai Gu[b], Jhuma Sadhukhan[a,b,*]

[a] Centre for Environment and Sustainability, University of Surrey, Guildford, Surrey GU2 7XH, UK
[b] Department of Chemical and Process Engineering, University of Surrey, Guildford, Surrey GU2 7XH, UK
[c] School of Engineering, Newcastle University, Newcastle Upon Tyne, Tyne and Wear NE1 7RU, UK
[d] School of Natural and Environmental Sciences, Newcastle University, Newcastle upon Tyne, Tyne and Wear NE1 7RU, UK

GRAPHICAL ABSTRACT

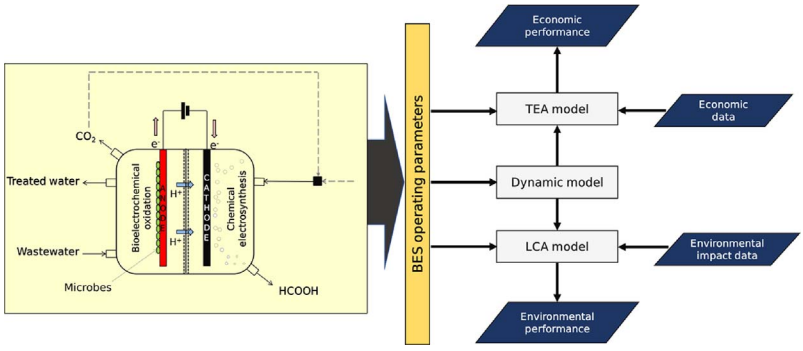

ARTICLE INFO

Keywords:
Resource recovery and productivity from waste
Technical systems for policy
Circular economy
Electrochemical biorefinery
Carbon dioxide capture and reuse

ABSTRACT

A novel framework, integrating dynamic simulation (DS), life cycle assessment (LCA) and techno-economic assessment (TEA) of a bioelectrochemical system (BES), has been developed to study for the first time wastewater treatment by removal of chemical oxygen demand (COD) by oxidation in anode and thereby harvesting electron and proton for carbon dioxide reduction reaction or reuse to produce products in cathode. Increases in initial COD and applied potential increase COD removal and production (in this case formic acid) rates. DS correlations are used in LCA and TEA for holistic performance analyses. The cost of production of HCOOH is €0.015–0.005 g^{-1} for its production rate of 0.094–0.26 kg yr^{-1} and a COD removal rate of 0.038–0.106 kg yr^{-1}. The life cycle (LC) benefits by avoiding fossil-based formic acid production (93%) and electricity for wastewater treatment (12%) outweigh LC costs of operation and assemblage of BES (−5%), giving a net 61MJkg^{-1} HCOOH saving.

1. Introduction

Research interest in renewable fuels has intensified over the last two decades due to the finiteness of fossil fuels and concern about their environmental issues (IPCC, 2014). Lately, there has been a particular focus on the production of renewable fuels and chemicals from waste, as it does not only enable the reuse of an otherwise insignificant stream to maximise utility but also capacitates the realisation of a circular

* Corresponding author at: Centre for Environment and Sustainability, University of Surrey, Guildford, Surrey GU2 7XH, UK.
E-mail address: j.sadhukhan@surrey.ac.uk (J. Sadhukhan).

https://doi.org/10.1016/j.biortech.2018.01.071
Received 6 November 2017; Received in revised form 12 January 2018; Accepted 15 January 2018
Available online 04 February 2018

Nomenclature

q	COD Consumption rate in the biofilm (kgCOD kgVS^{-1} day^{-1}), VS = Volatile solids as a measure of biomass
S_D	COD (substrate) concentration (kgCOD cm^{-3})
ϕ_a,ϕ_i	volumetric fraction of active and inactive biomass (dimensionless)
R,F	universal gas constant and Faraday constant
v	advective velocity (cm^{-2} day^{-1})
r_{res}	specific rate of endogenous respiration (day^{-1})
$D_{ED,f}$	diffusion coefficient of substrate in the biofilm (cm^2 day^{-1})
ρ_a,ρ_i	density of active and inactive biomass (kgVS cm^{-3})
j	current density (mA cm^{-2})
	biofilm conductivity (Sm^{-1})
γ_1	electron equivalence of substrate
τ	time conversion factor (s day^{-1})
V_1,V_2	constants of the linear applied potential-related function
r_{dec}	rate of active biomass inactivation (day^{-1})
R_{HCOOH}	rate of formic acid production (mg L^{-1} hr^{-1})
FE_{HCOOH}	Faradic efficiency for formic acid production (%)
n	number of electrons transferred per mole of formic acid
J_{SD}	molar flux of substrate passing through the biofilm (kgCOD cm^{-2} day^{-1})
C_i	total initial capital investment
β	cost avoided from an activated sludge plant for equivalent COD removal
O_n	annual operating cost
T_n	annual income tax
$q_{\max}$	maximum consumption rate in the biofilm (kgCOD kgVS^{-1} day^{-1})
K_{SD}	half maximum rate concentration (KgCOD cm^{-3})
η	local electric potential of the biofilm (V)
T	temperature (298.15 K)
E_{KA}	half maximum rate potential (V)
b_{res}	endogenous decay coefficient of active biomass (day^{-1})
$D_{ED,l}$	diffusion coefficient of substrate in the bulk liquid (cm^2 day^{-1})
L,L_f	thickness of diffusion layer and biofilm (cm)
Q_s	general source term (mA cm^{-3})
f_0^e	fraction of energy generating electrons (dimensionless)
γ_2	electron equivalence of biomass
Y	true yield (kgVS kgCOD^{-1})
V_{app}	applied cell potential (V)
b_{dec}	first-order inactivation rate coefficient (day^{-1})
A_{an},A_{cat}	Anode and Cathode surface area (cm^2)
V_{an},V_{cat}	Anode and Cathode compartment volume (cm^3)
M_w	molecular weight of acetate (g mol^{-1})
z	Spatial longitudinal coordinate from the anode surface (cm)
θ	HCOOH selling price
t	number of operational years
r	required rate of return
$(\hat{\theta})$	HCOOH selling minimum price

economy. At the same time, environmental pollution and waste generation in the industrial, municipal and agricultural sectors continue to grow (Pant et al., 2011). For example, the pollution of aquatic ecosystems by industrial and municipal wastewaters, containing metallic and organic contaminants, is a growing environmental concern. The accumulation of these contaminants in aquatic ecosystems poses a toxicological hazard to public health and communities of dependent living organisms. Moreover, traditional wastewater treatment methods significantly contribute to greenhouse gas (GHG) emissions globally (IPCC, 2014). Global GHG emissions from conventional wastewater treatment plants could, in fact, reach about 12.1 ktd^{-1} by 2025 (Rosso and Stenstrom, 2008). Thus, innovative wastewater treatment technologies with synergetic resource recovery and transformation capabilities are currently being developed (Puyol et al., 2017).

One of such technologies, bioelectrochemical systems (BESs), present a promising opportunity for wastewater treatment and simultaneous *in-situ* electricity, fuel and chemical production (Sadhukhan et al., 2016) as well as metal recovery (Ng et al., 2016). BESs are electrochemical devices that are aided by pure cultures, bacteria communities or isolated enzymes for catalysing redox reactions (Rabaey et al., 2009). In a typical BES setup, wastewater is fed to the anodic chamber, where its organic contaminants are oxidised to produce CO_2, protons and electrons. Depending on the mode of operation, the electrons travel through a circuit to either solely generate electricity or combine with CO_2 or other substrates and protons (which diffuse through a membrane) to produce fuels or chemicals in the cathodic chamber. Various operational modes of BESs, including microbial fuel cells (MFCs), microbial electrolysis cells (MECs), microbial electrosynthesis systems and other variants have been trialled with promising results (Rozendal et al., 2008). These BESs are targeted towards various applications, notably remote electricity generation and wastewater treatment, resource recovery, sensor applications, desalination and electrochemical reduction of CO_2 into high-value chemical compounds (Bajracharya et al., 2016). Among these applications, the synthesis of chemical compounds *via* CO_2 reduction offers multifunctional benefits towards the implementation of several the United Nations' Sustainable Development Goals (SDGs), such as SDG 6: clean water and sanitation; SDG 7: affordable and clean energy, and SDG 13: climate action (Sadhukhan et al., 2018). These benefits include wastewater treatment through the removal of chemical oxygen demand (COD), renewable energy production from electrons liberated from the wastewater and temporary storage and utilisation of CO_2 (a potent GHG) to synthesise chemical products otherwise produced from fossil fuels (Shemfe et al., 2018).

Several valuable chemical compounds, including methane, formic acid, acetic acid, propanol, butanol and ethanol, can be produced from BESs *via* CO_2 reduction at different reduction potentials (Sadhukhan et al., 2016). Formic acid (HCOOH) stands out from other feasible chemical products due to its versatility. It is used as a chemical feedstock in the textile, pharmaceutical and food preservative industries, a liquid carrier for safe hydrogen storage and transportation, and fuel for fuel cells (IHS Markit, 2017; Kim et al., 2009; Rice et al., 2002). The global production of HCOOH has reached 620 kt in 2012, and it is projected to exceed 760 kt by 2019 at an average annual growth rate of 3.8% (Pérez-Fortes et al., 2016). Despite the versatility of HCOOH, it is primarily produced industrially from resource-intensive and environmentally damaging fossil-based methods, decarboxlative cyclization of adipic acid, oxidation of butane and hydrolysis of methyl formate (Ecoinvent, 2013). Thus, a BES-based production route, considering its plausible relative environmental benignity, could potentially replace current fossil-based production methods (Sadhukhan, 2017). To this end, only one technical and sustainability analysis study exists. Sadhukhan (2017) has investigated sustainable development of BES, encompassing technical modelling by analytically solving partial differential equations and triple-bottom-line life cycle sustainability assessment, applied to wastewater treatment in anode and formic acid synthesis in cathhode.

In a typical BES setup, at pH = 7 Normal Hydrogen Electrode, the open circuit potential for COD oxidation (acetate) at bioanode is ~ −0.3 V (Call and Logan, 2008). However, CO_2 reduction to HCOOH requires a potential of at least −0.41 V (Rabaey and Rozendal, 2010). As the resulting cell potential (−0.41 − (−0.3) = −0.11 V) is

negative, the reaction is non-spontaneous and requires external electrical energy input. Nevertheless, in real systems, a higher voltage (> 0.4 V) than the theoretical requirement of −0.11 V is required for HCOOH production due to losses from cell overpotential (Zhao et al., 2012a). The additional power needed for HCOOH synthesis in the BES can be either supplied by an external power source or harvested from a single or stack of MFCs connected in series to the BES (Zhao et al., 2012b). Past experimental studies have reported the selective electrochemical reduction of CO_2 into HCOOH, driven by an external power source, on various metallic electrocatalysts, including Hg, Pb, Ti, In, Sn, Cd and Bi with Faradic efficiency of 77–97.4% (Alvarez-Guerra et al., 2014; Hori et al., 1994; Köleli and Balun, 2004). Zhao et al. (2012a) also demonstrated the production of HCOOH from CO_2 in a BES by utilising electricity generated from a series of MFCs with Pb electrodes and reported a maximum Faradic efficiency of 70%. Wang et al. (2015) found that using a two-layer rolled Sn-loaded gas diffusion electrode as a BES cathode, can reduce the requisite external electricity for the electrochemical reduction of CO_2 to HCOOH.

The prospect of producing HCOOH industrially, as suggested by these experimental studies, necessitates a complementary modelling framework to study the operational, economic and environmental performance of BES, which can be evaluated *via* dynamic simulation (DS), techno-economic assessment (TEA) and life cycle assessment (LCA), respectively. Prior DS studies have focused on the production of electricity and hydrogen (Karimi Alavijeh et al., 2015; Pinto et al., 2011). Also, limited studies are available on LCA of BES. Pant et al., 2010 proposed a systematic methodology and recommendations for performing the LCA of BES. Foley et al. (2010), conducted a comparative LCA of electricity generation and hydrogen peroxide production from BES and biogas generation from anaerobic digestion. TEA studies of BES are likewise scanty in literature. In a prior economic assessment by Rozendal et al. (2008), the capital costs of lab-scale BES for wastewater treatment and electricity generation or hydrogen production were evaluated. Christodoulou and Velasquez-Orta (2016) compared the production costs of acetic acid production from the microbial electrochemical reduction of CO_2 and anaerobic fermentation of CO. However, there is no methodological framework in existing literature that integrates LCA, TEA and DS of BES to enable holistic optimisation of its operation. The integration of DS, TEA and LCA into a framework, a challenge yet to be confronted, is much needed, as temporal and spatial BES inputs will profoundly impact its economic and environmental performance. This paper thus aims to meet this challenge by presenting the first ever integrated LCA, TEA and DS framework to study the performance of BES for simultaneous wastewater bioremediation and formic acid production, as the first proof of concept.

2. Methods

2.1. System description

Fig. 1 shows the schematic of the proposed BES—a dual chamber BES. It has both anodic and cathodic chambers, separated by a cation exchange membrane, and features a bioanode and an indium-based cathode.

In the anodic chamber, electrons, protons and CO_2 are liberated from the wastewater COD *via* microbial oxidation. The protons diffuse through the cation exchange membrane to the cathodic chamber, while the electrons, supplemented by an external electric power supply, goes through a circuit to the cathode. Furthermore, it is assumed that the CO_2 released from the anodic chamber is recycled to the cathodic chamber, which contains 0.1 M $KHCO_3$ catholyte. The protons, electrons and CO_2 finally combine in the cathodic chamber to synthesise HCOOH.

2.2. Dynamic modelling

The dynamic model describes the relationship between bacterial kinetics, substrate concentration (COD) and the electric potential at the bioanode, whereas the HCOOH production rate at the cathode is calculated based on the current density and the Faradic efficiency of the electrode. The dynamic model is based on the conductive biofilm matrix approach proposed by Marcus et al., (2007). The conductivity of the matrix is linked to the current density and local voltages along the biofilm depth. A similar model has also been used previously (Karimi Alavijeh et al., 2015) to describe the bioanode of MEC, where the current density is subsequently used to calculate the hydrogen production rate. The assumptions made in this model are similar to those described in previous studies (Marcus et al., 2007; Karimi Alavijeh et al., 2015), as follows:

1. The biofilm is assumed to be a conductive matrix, with a fixed conductivity .
2. Electron transfer occurs *via* direct conduction mechanism through the biofilm.
3. A concentration boundary layer is assumed adjacent to the biofilm layer and exhibits linear concentration profiles.
4. Voltage loss during electron transfer from conductive biofilm to the anode and during ion transfer across the membrane is assumed to be negligible.
5. pH and temperature are considered to be constant throughout the system.
6. Acetate is assumed to be the 'model electron donor' substrate present in the wastewater.
7. Protons at the cathode are assumed to be only consumed in HCOOH production and no other process.

As wastewater enters the anodic chamber, the substrate (COD) is oxidised by the biomass. Based on the Nernst-Monod model proposed by Marcus et al. (2007), the specific rate of COD utilisation or substrate consumption in the biofilm (q) is given as:

$$q = q_{\max}\phi_a\left(\frac{S_D}{S_D + K_{SD}}\right)\left(1 \Big/ \left(1 + \exp\left[-\frac{F}{RT}\eta\right]\right)\right) \quad (1)$$

where $q_{\max}$,ϕ_a,S_D,K_{SD},η,F,R *and* T represent the maximum specific substrate consumption rate, volumetric fraction of active biomass, substrate concentration, half maximum rate substrate concentration, local electric potential relative to E_{KA} (half maximum rate potential), Faradic constant, Universal gas constant and temperature, respectively. The biomass also undergoes endogenous respiration at a specific rate (r_{res}) as follows:

$$r_{res} = b_{res}\phi_a\left(1 \Big/ \left(1 + \exp\left[-\frac{F}{RT}\eta\right]\right)\right) \quad (2)$$

where b_{res} is the endogenous self-oxidation coefficient for active

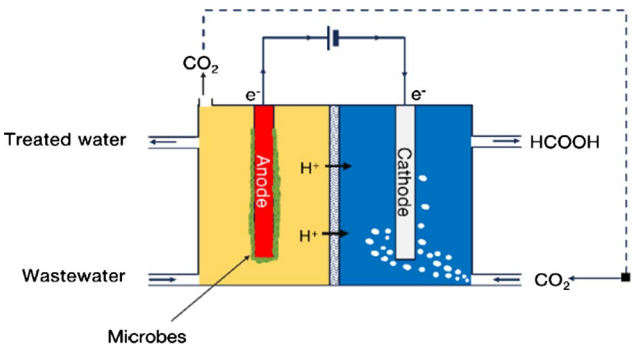

Fig. 1. BES schematic under consideration.

biomass. Mass balance of substrate in the biofilm is given as:

$$0 = D_{ED,f}\frac{\partial S_D}{\partial z^2} - \rho_a q \tag{3}$$

where $D_{ED,f}$ *and* ρ_a represent the corrected diffusion coefficient of the substrate in the biofilm and density of active biomass, respectively. Eq. (3) is solved using two boundary conditions, one at the anode surface ($z = 0$) and the other at the interface of biofilm and the diffusion layer ($z = L_f$).

$$D_{ED,f}\frac{\partial S_D}{\partial z}\bigg|_{z=0} = 0; \tag{4}$$

$$D_{ED,l}\frac{\partial S_D}{\partial z}\bigg|_{z=L_f} = D_{ED,f}\frac{\partial S_D}{\partial z}\bigg|_{z=L_f} = \left(\frac{D_{ED,l}}{L}\right)(S_{D,bulk} - S_{D,surface}) \tag{5}$$

where $D_{ED,l}$,L,$S_{D,bulk}$ *and* $S_{D,surface}$ represent the substrate diffusion coefficient in the bulk liquid, the thickness of the diffusion layer, substrate concentration in the bulk liquid and substrate concentration at the biofilm interface, respectively.

It is assumed that the only factor that can change the substrate concentration in the bulk liquid is the consumption of substrate in the biofilm.

$$V_{an}\left(\frac{dS_{D,bulk}}{dt}\right) = -A_{an}J_{SD} \tag{6}$$

where V_{an},A_{an} $and J_{SD}$ represent the anodic chamber volume, anode surface area and molar flux of substrate passing through the biofilm, respectively.

Ohm's law is used to calculate the current density.

$$\nabla \cdot j = Q_s \quad \text{with} \quad j = -k_{bio}\nabla\eta = -k_{bio}\frac{d\eta}{dz} \tag{7}$$

$$-k_{bio}\frac{d^2\eta}{dz^2} = Q_s = -\frac{F\gamma_1}{\tau}f_e^0\rho_a q - \frac{F\gamma_2}{\tau}\rho_a r_{res} \tag{8}$$

where j,Q_s,k_{bio},γ_1,γ_2,τ *and* f_0^e represent the current density, general source term, biofilm conductivity, electron equivalence of substrate, electron equivalence of active biomass, time conversion ($86{,}400\ \mathrm{s\ day^{-1}}$) and fraction of electrons from the substrate used for energy generation respectively. The potential equation is solved using the following boundary conditions at $z = 0$ and $z = L_f$:

$$\eta|_{z=0} = V_1 \cdot V_{app} - V_2 - E_{KA} \tag{9}$$

and

$$\frac{d\eta}{dz}\bigg|_{z=L_f} = 0 \tag{10}$$

where V_{app} represents the applied potential and V_1 *and* V_2 represent the constants of linear applied potential related function (Karimi Alavijeh et al., 2015).

The active biomass gets inactivated at the following rate:

$$r_{dec} = b_{dec}\phi_a \tag{11}$$

where b_{dec} is the inactivation rate coefficient.

In addition to the active bacteria, which contribute to COD consumption, this model also includes a diffusive non-conductive layer (made up of inactive microbes) between the conductive matrix and the bulk anodic liquid. The rate of change of active and inactive biomass are given as:

$$\frac{\partial\phi_a}{\partial t} + \frac{\partial(v\phi_a)}{\partial z} = Yq - r_{res} - r_{dec} \tag{12}$$

and

$$\frac{\partial\phi_i}{\partial t} + \frac{\partial(v\phi_i)}{\partial z} = \frac{\rho_a}{\rho_i}r_{dec} \tag{13}$$

Table 1
Parameter values used in the dynamic model.

Parameter	Value	Ref.
q_{max} ($\mathrm{day^{-1}}$)	7.92	Marcus et al. (2007)
b_{res} ($\mathrm{day^{-1}}$)	0.05	Marcus et al. (2007)
L(cm)	0.01	Marcus et al. (2007)
Y ($\mathrm{kgVS\ kgCOD^{-1}}$)	0.228	Kaewsuk et al. (2010)
γ_1 ($\mathrm{mol\ e\text{-}kgCOD^{-1}}$)	125	Karimi Alavijeh et al. (2015)
k_{bio} ($\mathrm{S\ m^{-1}}$)	0.05	Karimi Alavijeh et al. (2015)
F ($\mathrm{C\ mol^{-1}}$)	96,485	
A_{an},A_{cat} ($\mathrm{cm^2}$)	16	Zhao et al. (2012b)
ρ_a,ρ_i ($\mathrm{kgCOD\ m^{-3}}$)	300	Karimi Alavijeh et al. (2015)
K_{SD} ($\mathrm{kg\ m^{-3}}$)	0.174	Kaewsuk et al. (2010)
b_{ina} ($\mathrm{day^{-1}}$)	0.05	Marcus et al. (2007)
$D_{ED,l}$ ($\mathrm{cm^2\ day^{-1}}$)	0.941	Marcus et al. (2007)
$D_{ED,f}$ ($\mathrm{cm^2\ day^{-1}}$)	0.753	Marcus et al. (2007)
γ_2 ($\mathrm{mol\ e^-\ kgVS^{-1}}$)	125	Karimi Alavijeh et al. (2015)
f_0^e	0.9	Marcus et al. (2007)
R ($\mathrm{J\ mol^{-1}\ K^{-1}}$)	8.314	
V_{an},V_{cat} ($\mathrm{cm^3}$)	290	Zhao et al. (2012b)
FE_{HCOOH} (%)	94.9	Hori et al. (1994)

where v, Y and ϕ_i represent the advective velocity, true yield and volumetric fraction of inactive biomass, respectively.

The advective velocity of the biofilm matrix is given as:

$$\frac{\partial v}{\partial z} = Yq - r_{res} - r_{dec} - \frac{\rho_a}{\rho_i}r_{dec} \tag{14}$$

HCOOH production rate at the cathode is calculated based on the current density, cathode surface area, cathode chamber volume and the Faradic efficiency of the electrode:

$$R_{HCOOH} = \frac{jA_{cat}FE_{HCOOH}M_w}{nFV_{cat}} \tag{15}$$

where A_{cat},FE_{HCOOH},M_w,n *and* V_{cat} represent the cathode surface area, Faradic efficiency of the cathode, the molecular weight of HCOOH, number of electrons transferred per mole of HCOOH ($n = 2$) and volume of the cathodic chamber, respectively. The dynamic model described above is solved using the input parameters provided in Table 1 to determine the rate of change of COD (substrate concentration), HCOOH production rate, the rate of change of active and inactive biomass in the biofilm and the voltage and current density profiles.

2.3. Techno-economic assessment

The TEA methodology employed in this study involves the estimation of capital and operating costs, and in turn, the cost of production per unit of HCOOH synthesised (Sadhukhan et al., 2014). Firstly, the equipment cost of the BES components, including anode, cathode, membrane and current collectors, are calculated using the cost parameters obtained from literature and commercial manufacturers (Table 2). The resulting equipment cost (C_e) is multiplied by a Lang factor (f_L) to compute the total capital cost (C_T), as shown in Eq. (16).

$$\text{Total capital cost } (C_T) = f_L.\ C_e; (f_L = 4.64) \tag{16}$$

Subsequently, the total operating cost, comprising costs of anolyte, catholyte, requisite external electricity and maintenance, is calculated using Eq. (17).

$$\text{Total operating cost } (O_T) = O_a + O_C + O_{elec} + O_{main} \tag{17}$$

The operating cost of the anolyte (O_a), catholyte (O_c) and requisite external electricity (O_{elec}) are estimated from current market prices (Table 2), while maintenance cost (O_{main}) is assumed to be 1% of the equipment cost.

The resulting total capital and operating costs are then used as inputs for the estimation of the cost of production per unit of HCOOH

Table 2
Parameters for BES components and operating inventory cost estimation.

Parameter	Material	Unit	€/unit	Ref.
Capital cost components				
Anode	Carbon cloth	m^2	14.43	PRF composites, 20301A
Membrane	Nafion	m^2	444	Rozendal et al. (2008)
Cathode	In/C- (20 wt %)	m^2	15	Estimated from In/C – (20 wt%)
Current collector[a]	Cu	m^2	27.5	Rozendal et al. (2008)
Operating cost components				
Anolyte[b]	Acetate	m^3	0.00113	
Catholyte[c]	0.1 M $KHCO_3$	m^3	0.5254	
Requisite external energy	Electricity	kWh	0.1413	Average UK market price (Sadhukhan et al., 2014).
Maintenance	$0.01C_e$			

[a] Area of current collector = 0.005 m^3.
[b] Assumed from similar wastewater stream.
[c] Catholyte unit cost estimated from the mass of $KHCO_3$ solute.

synthesised (C_P), as given in Eq. (18).

$$C_P = \frac{(C_T + R_T)\gamma + O_T - \beta}{m} \quad (18)$$

Capital recovery factor (γ) is estimated using Eq. (19).

$$\gamma = \frac{r}{1-(1+r)^t} \quad (19)$$

The operational years (t) and discount rate (r) are taken as 20 years and 10%, respectively (Sadhukhan, 2017). Furthermore, it is assumed that the BES is replaced every five years, and this is the basis for equipment replacement cost (R_T) estimation. The annual HCOOH yield (m) is estimated from DS results using 1 gL^{-1} COD and 0.9 V applied voltage as the basis for estimation. The annual energy cost avoided for equivalent COD removal in an activated sludge (AS) plant (β) is also estimated from DS results (1 gL^{-1} COD and 0.9 V basis), and an AS plant energy requirement of 2 Wh per gCOD (Xu et al., 2017).

2.4. Life cycle assessment

The LCA has been conducted in four phases: (i) goal and scope definition (ii) inventory analysis; (iii) impact assessment and (iv) interpretation, in line with ISO standards: 14040, 14041 and 14044 (ISO, 2006a,b, 1998).

2.4.1. Goal and scope of study

The goal of this study is to assess the environmental impact of BES-synthesised HCOOH. The functional unit is thus 1 kg of HCOOH. As the BES is bifunctional (i.e. COD removal and HCOOH synthesis), 1 kg HCOOH formation is associated with the removal of 0.406 kg COD, (obtained from DS results shown later in Table 4). The scope of the LCA spans from the 'cradle' (raw material extraction) to the production gate in accordance with the system boundary adopted for the TEA in Section 2.3. The system boundary, encompassing raw material extraction, material processing of BES components and operating inventory, is illustrated in Fig. 2.

2.4.2. Inventory analysis

Inventory data are from Ecoinvent database 3.0 (Ecoinvent, 2013) as provided in SimaPro 8.2.3.0 and results from the dynamic model (described in Section 2.2). Ecoinvent database pertaining to Great Britain (GB) has been used for the inventory analysis; otherwise, the EU (RER) or global (GLO) proxies have been employed. Table 3 shows the corresponding Ecoinvent 3.0 database for the inventory items as well as

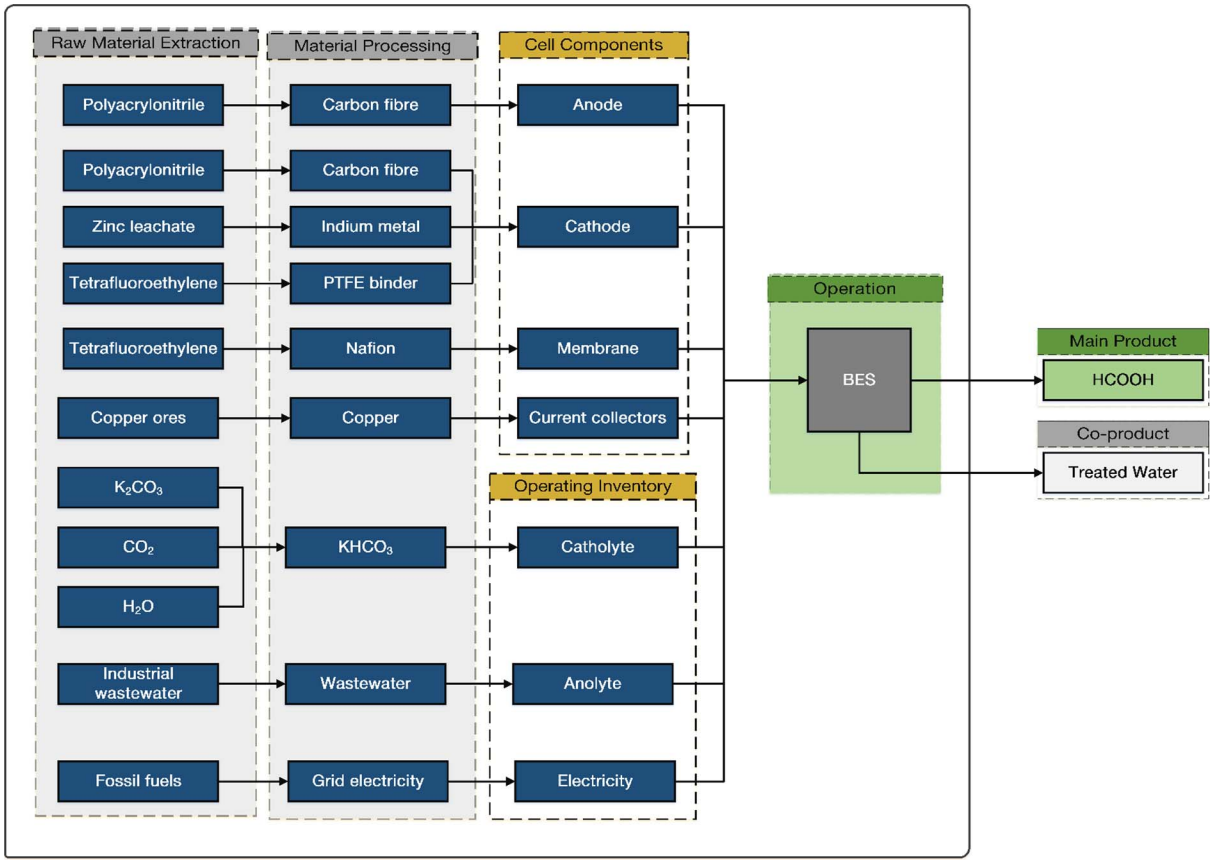

Fig. 2. Raw material extraction, BES components manufacturing and operations within the LCA system boundary.

Table 3
Ecoinvent 3.0 databases for BES components' and operating inventory.

LCA stage	Item	Amount	Unit	Ecoinvent 3.0 database
BES components	Anode	0.24	mg	Carbon fibre [0.24 mg] Inputs for Carbon fibre[1 kg]: Water, completely softened, from decarbonised water, at user {RER}| production [3.39 kg]; Acrylonitrile {RER}| Sohio process [1 kg]; *N,N*-dimethylformamide {RER}| production [0.01 kg]; Nitrogen, liquid {RER}| air separation, cryogenic [5.33 kg]; Oxygen, liquid {RER}| air separation, cryogenic [1.62 kg]; Heat, in chemical industry {RER}| steam production in chemical industry [18.43 MJ]; Electricity, high voltage {GB}| electricity production, natural gas, conventional power plant [2.38 kWh] (GaBi, 2016) Emissions from Carbon fibre [1 kg] Oxygen [1.22 kg]; Nitrogen [10.44 kg]; Dimethyl formamide [0.0097 kg]; Carbon dioxide [1.01 kg]; Carbon monoxide [0.00324 kg]; Nitrogen dioxide [0.0038 kg]; Hydrogen cyanide [0.0031 kg]; Ethane [0.0000101 kg]; Ammonia [0.00116 kg]; Sulfuric acid [0.02 kg]; Water, GB [8099 m^3]
	Cathode	0.34	mg	Inputs for In-based cathode [1 kg]: Indium {RER} production [0.2 kg]; Tetrafluoroethylene {RER} production [0.1 kg]; Carbon Fibre [0.8 kg]
	Membrane	0.28	mg	Tetrafluoroethylene {RER} production
	Current collectors	0.55	mg	Copper, from solvent-extraction electro-winning {GLO}| copper production, solvent-extraction electro-winning
Operating inventory	Requisite electrical energy	0.92	MJ	Electricity, high voltage {GB}| production mix
	Catholyte	1.38	kg	Potassium bicarbonate {GLO}| production, from potassium hydroxide
COD-avoided energy (COD benefit)		2.92	MJ	Electricity, high voltage {GB}| production mix

the amounts of the items. The collated inventory items include BES components: membrane, anode, cathode and current collectors, the operating inventory: requisite external electricity for HCOOH synthesis and catholyte and the avoided energy for COD removal. It is assumed that the system utilises a Nafion membrane, which is manufactured from polytetrafluoroethylene. Inventory data for tetrafluoroethylene provided in Ecoinvent 3.0 has been used as a proxy for Nafion. The anode is made out of carbon fibre, which is manufactured from polyacrylonitrile. The inventory data for carbon fibre has been collated from GaBi 6.0 Ecoinvent 3.0, and equivalents in Simapro Ecoinvent 3.0 have

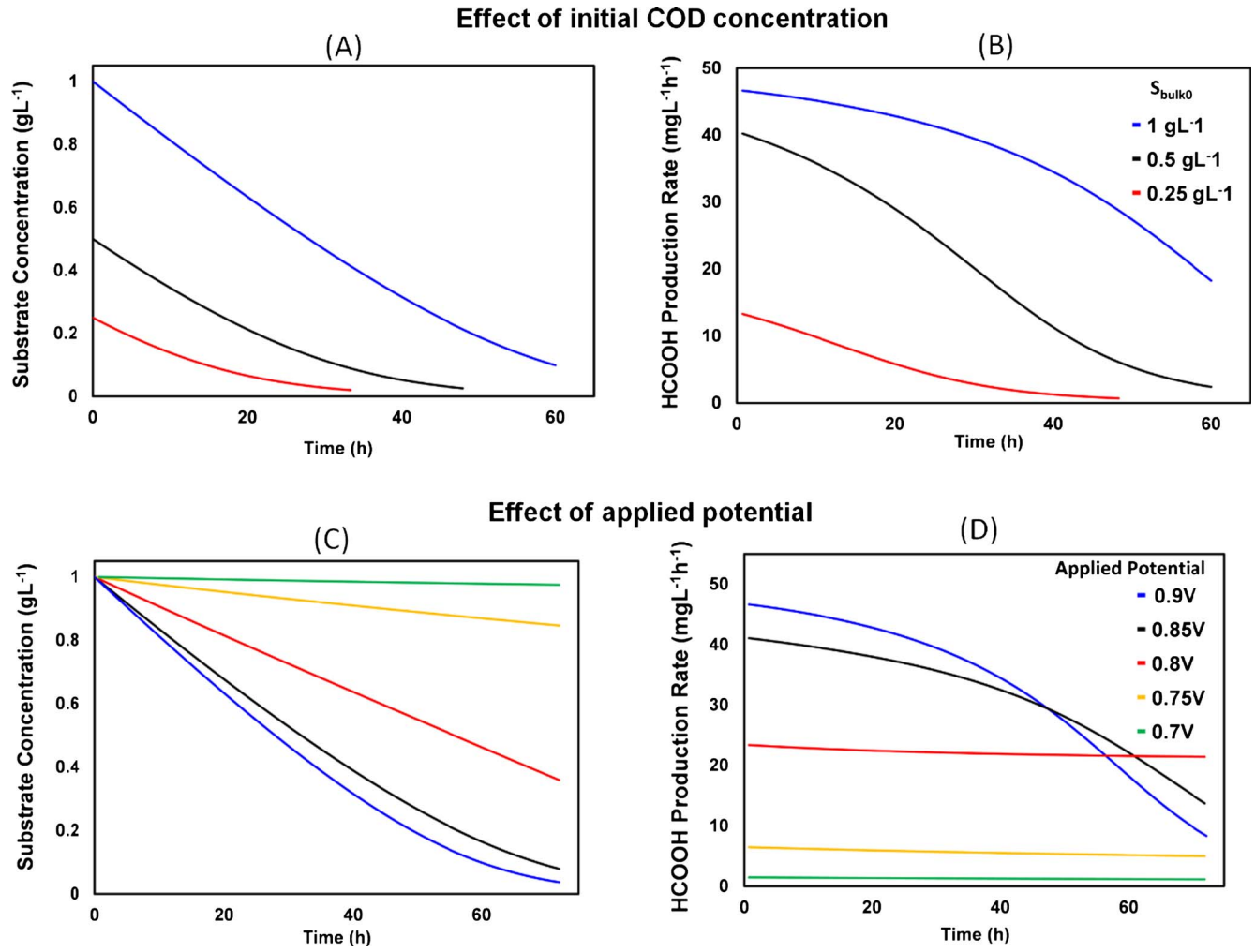

Fig. 3. Change in substrate concentration (gL^{-1}) and HCOOH production rate ($mgL^{-1}h^{-1}$) as a function of time for three different values of initial COD concentration (A & B), S_{bulk0} = 1, 0.5 and 0.25 gL^{-1} and for five different applied potential values (C & D), V_{app} = 0.9 V, 0.85 V, 0.8 V, 0.75 V and 0.7 V. The effect of initial COD concentration has been studied at a fixed applied potential of 0.9 V, and the effect of applied potential has been studied at a fixed initial COD concentration of 1 gL^{-1}.

been used accordingly. The inventory data for the indium-based cathode has been obtained by assuming 18 wt%, 73 wt% and 9 wt% for the indium catalyst, carbon fibre support and polytetrafluoroethylene binder, respectively. The current collectors are made from copper, which is manufactured from solvent-extraction electro-winning. The requisite external electricity for HCOOH synthesis, estimated from the DS, is assumed as high voltage grid mix in Great Britain. The catholyte (0.1 M $KHCO_3$) has also been accounted for based on data provided in Ecoinvent database 3.0. A catholyte make-up factor of 0.5% is assumed in this study, although in an ideal industrial case the catholyte is expected to be fully recovered. This assumption is consistent with a recent TEA on electrochemical conversion (Dang et al., 2017). Avoided electricity for equivalent COD removal by an activated sludge plant is estimated to be 3.21 $kWhkg^{-1}$ (consumption of energy per kg of COD removed *via* activated sludge in Europe) (Guerrini et al., 2017), for which the chosen inventory database is high voltage grid mix in Great Britain in Ecoinvent 3.0. HCOOH is industrially produced by three fossil-based methods: decarboxylative cyclization of adipic acid, oxidation of butane and hydrolysis of methyl formate (Ecoinvent, 2013). An average of these production methods is considered for comparison with the BES-synthesised HCOOH.

2.4.3. Life cycle impact assessment

IMPACT 2002+, as provided in SimaPro 8.2.3.0, is employed for life cycle impact assessment (LCIA). This methodology allows the combined assessment of midpoint and endpoint impact categories. The midpoint impact categories include carcinogens, non-carcinogens, respiratory inorganics and organics, ionising radiation, ozone layer depletion, aquatic ecotoxicity, terrestrial ecotoxicity, terrestrial acidification, land occupation, aquatic acidification, aquatic eutrophication, global warming, non-renewable energy and mineral extraction (Humbert et al., 2012). These midpoint categories are then classified into four endpoint impact categories: human health, ecosystem quality, climate change, and resources.

Firstly, the midpoint environmental impacts (MEI) of the BES components, operating inventory and COD removal, have been individually assessed (Fig. 2). Next, the MEI of equal mixes of the three fossil-based formic acid production methods are estimated. The potential net MEI saving is estimated as (i.e. MEI benefit – MEI cost) (Sadhukhan, 2017; Sadhukhan et al., 2014). In the net MEI saving analysis, in one case, avoided burden is estimated based on COD removal or HCOOH production alone. In another case, the avoided burden is allocated to the two services, i.e. COD removal and HCOOH production, based on their economic allocations (Sadhukhan et al., 2014). Lastly, the MEIs of BES components and operating inventory and conventional fossil-based COD removal and formic acid production methods are classified and characterised into endpoint environmental impacts for net MEI savings.

3. Results and discussion

3.1. Dynamic simulation results

- The dynamic model is used to determine the influences of the applied potential and the initial COD concentration in the wastewater on the substrate consumption (COD removal) rate and HCOOH production rate. These results are presented in Fig. 3A and B. The tabulated results of the influences of the initial COD concentration in the wastewater and the applied potential on the substrate consumption (COD removal) rate and HCOOH production rate are also presented in Tables 4A and 4B, respectively.

3.1.1. The influence of initial COD concentration on COD removal and HCOOH production

As can be seen from Fig. 3A and B, change in the initial COD (substrate) concentration (S_{bulk0}) has a strong influence on the rates of substrate consumption and HCOOH production. For three values of S_{bulk0}: 1 gL^{-1}, 0.5 gL^{-1}, and 0.25 gL^{-1}, 90% of substrate consumption took about 60 h, 40.5 h and 31 h, respectively. Calculating based on the total amount of substrate consumed, the rate of substrate consumption per hr is highest at $S_{bulk0} = 1\ gL^{-1}$ (15 $mgL^{-1}h^{-1}$), followed by 0.5 gL^{-1} (11 $mgL^{-1}h^{-1}$) and 0.25 gL^{-1} (7 $mgL^{-1}h^{-1}$). The rate of HCOOH production also follows the same trend as can be seen in Fig. 3B. For all the three values of S_{bulk0}, HCOOH production rate decreases with time with a corresponding decrease in the available substrate for oxidation at the bioanode. Starting HCOOH production rates in this analysis for S_{bulk0}, 1 gL^{-1} and 0.5 gL^{-1} are about 46 and 40 $mgL^{-1}h^{-1}$. These values are comparable to those obtained by Chen et al. (2013), 63 $mgL^{-1}h^{-1}$; but higher than those obtained by Zhao et al. (2012a), 21 $mgL^{-1}h^{-1}$. It should be noted that Zhao et al. (2012a) have used composite modified cathode which had an average Faradic efficiency of about 75%. In this study, an indium-based cathode is assumed with a Faradic efficiency of 94.9% (Hori et al., 1994). Some other factors which have not been included in the dynamic model, such as the overpotential at the cathode and the losses due to membrane resistance may decrease the current density in real systems and thereby the HCOOH production rate.

3.1.2. The influence of applied potential on COD removal and HCOOH production

Fig. 3C and D show the influence of applied potential on substrate concentration and HCOOH production rate. As can be seen in Fig. 3C, the rate of substrate consumption increases quite linearly with increase in applied potential, between 0.7 V and 0.9 V. Substrate consumption rate per hour can be calculated from Fig. 3C and increases from, 0.3 $mgL^{-1}h^{-1}$ for $V_{app} = 0.7$ V to reach up to 15 $mgL^{-1}h^{-1}$ for $V_{app} = 0.9$ V. HCOOH production rate at the start, also follows a linear trend with applied potential with the highest at 0.9 V and lowest at 0.7 V. Zhao et al. (2012a,b) also observed a linear dependence between HCOOH production rate and applied potential. However, as it can be seen in Fig. 3D, this linear trend breaks after about 40 h, due to the complex interdependence between the substrate concentration and the current density (as described in Eqs. (1), (3) and (7)). A faster-decreasing substrate concentration for 0.9 V results in a proportionate decrease in current density. This causes the HCOOH production rate for 0.9 V to fall below that of 0.85 V and 0.8 V. Near the end of 3 days (72 h), the HCOOH production rate is highest for 0.8 V, which remains constant roughly at an average value of 22 $mgL^{-1}h^{-1}$. The overall HCOOH production in one batch would still be highest for 0.9 V applied potential. It should also be noted here that the Faradic efficiency is known to have a nonlinear relationship with applied potential (Zhao et al. 2012a,b; Wang et al. 2015), which is mainly dependent on the type of material used for the cathode, amongst other factors. In this study, a constant Faradic efficiency is assumed. Thus a linear trend of HCOOH production is expected. LCA and TEA will address how the two important parameters: initial COD concentration and applied potential, as presented in Tables 4A and 4B, influence the environment and economic cost of running the proposed system.

Table 4A
Change in COD removal rate and HCOOH production rate due to change in initial COD (0.25–1.00 gL^{-1}) at a constant applied voltage of 0.9 V.

Initial COD (gL^{-1})	0.25	0.50	1.00
COD removal rate ($gL^{-1}h^{-1}$)	0.007	0.011	0.015
HCOOH production rate ($gL^{-1}h^{-1}$)	0.008	0.027	0.037
HCOOH production rate in gL^{-1} over 1 h	0.008	0.027	0.037
HCOOH production rate/COD removal rate	1.09	2.48	2.46
COD energy use/HCOOH production rate (kJg^{-1})	13.26	5.80	5.85
External power input W (Js^{-1})	0.003	0.003	0.003
External energy input/COD removal (kJg^{-1})	4.85	3.09	2.27
External energy input / HCOOH production rate (kJg^{-1})	4.47	1.24	0.92

Table 4B
Change in COD removal rate and HCOOH production rate due to change in applied voltage (0.7–0.9 gL^{-1}) at constant initial COD of 1 gL^{-1}.

Applied Voltage (V)	0.9	0.85	0.8	0.75	0.7
COD removal rate ($gL^{-1}\,h^{-1}$)	0.015	0.013	0.009	0.002	0.00030
HCOOH production rate ($gL^{-1}\,h^{-1}$)	0.037	0.032	0.022	0.005	0.0013
HCOOH production rate/ COD removal	2.46	2.50	2.47	2.72	4.17
External power input W (Js^{-1})	0.00274	0.00226	0.00122	0.00033	0.00007
External energy input in kJ over 1 h	0.010	0.008	0.004	0.001	0.0002
External energy input/COD removal (kJg^{-1})	2.266	2.160	1.705	2.052	2.760
External energy input/ production rate (kJg^{-1})	0.921	0.867	0.690	0.756	0.662

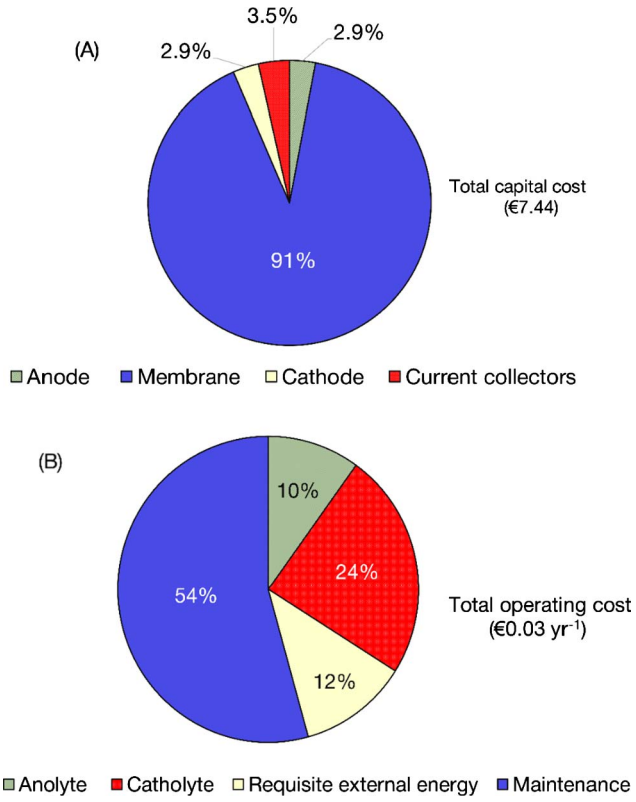

Fig. 4. A and B Total capital cost and total operating cost, respectively.

Table 5A
Total capital cost components.

Cost component	Size (cm^2)	Mass (mg)	Value (€)
Anode	16	0.0114	0.023
Cathode	16	0.0157	0.023
Membrane	20	0.0133	0.710
Current collectors (×2)	5	0.026	0.028
Equipment cost (×2)	–	–	1.57
Total capital cost	–	–	7.44

3.2. TEA results

The basis of TEA is derived from DS, 1 gL^{-1} COD and 0.9 V applied voltage (Table 4A). This corresponds to COD removal and HCOOH production rates of 0.0044 gh^{-1} and 0.0107 gh^{-1} (Table 4A), respectively. Accordingly, on an annual basis, HCOOH production rate and COD removal rate are estimated to be 0.094 $kgyr^{-1}$ and 0.038 $kgyr^{-1}$, respectively. Moreover, it is assumed that two BES units of 290 cm^3 each (Table 1) are set up. In this way, one unit will be operating while the other is regenerating so as to ensure continuous operation. The equipment cost, comprising the cost of anode, cathode, membrane, and current collectors (using cost data in Table 2), is estimated to be €1.57 (for two BES units). Fig. 4A shows the estimated equipment cost of the BES per component. Membrane cost accounts for 91% of the equipment cost, whereas anode, cathode, and current collectors' costs constitute 2.9%, 2.9% and 3.5%, respectively. Based on the calculated equipment cost of €1.57, the total capital cost for the system is €7.44 using equations 16. The total operating cost is €0.03 yr^{-1}, accruing from the costs of anolyte, catholyte, requisite external energy and maintenance, as shown in Fig. 4B. The catholyte cost forms the major constituent of the operating cost, at 54%, mainly due to the cost of the solute of 0.1 M $KHCO_3$. Tables 5A and 5B correspondingly show the cost breakup of the total capital and operating costs of the BES.

The production cost per unit mass of HCOOH produced is estimated as €0.015 g^{-1} using the values of total capital and operating costs presented in Tables 5A and 5B as inputs in Eq. (18). Future process improvements, in terms of durable high efficient metallic electrocatalysts or biocatalysts (microbial and enzymatic) and electrodes, will nullify the need for frequent component replacement and thus reduce the cost of production. Moreover, technological advances by way of devising highly efficient biocatalysts, electrodes or functional catalysts, in particular if these are recovered from waste streams *in-situ* (Sadhukhan et al., 2017), will improve the system's economic viability. To demonstrate, an increase in the HCOOH production rate by BES from 0.094 kg yr^{-1} to 0.26 kg yr^{-1}, will make its synthesis competitive at €0.005 g^{-1}. The modular characteristic of BES makes it favourable to scale-up by repeating an optimally sized module to meet a given throughput.

The influences of change in initial COD concentration of wastewater (at a constant applied potential of 0.9 V) and change in applied potential (at a constant initial COD of 1 gL^{-1}) on the cost of production per HCOOH produced are presented in Fig. 5A and 5B, respectively.

As can be seen in Fig. 5A, the cost of production noticeably decreases from €0.08 g^{-1} to €0.015 g^{-1} when the initial COD is increased from 0.25 to 1 gL^{-1}. An increase in applied potential from 0.75 to 0.90 V, on the other hand, also results in a striking reduction in the cost of production: €0.46 g^{-1} to €0.02 g^{-1}, due to increased productivity, as shown in Fig. 5B. This result suggests that applied voltage is a more crucial operating variable than initial COD (substrate concentration), within the studied operating envelope. Nevertheless, both variables: initial COD and applied potential should be optimised to reduce the cost of production. Furthermore, it appears that the cost of additional voltage to offset losses in real systems due to overpotentials may be somewhat minimal at a sufficiently high constant initial COD concentration.

3.3. LCA results

The midpoint environment impacts (MEI) of BES components, operating inventory, avoided energy for COD removal, average fossil-based HCOOH production, and the net MEI saving analysis results, are presented in Table 6. As can be seen in Table 6, the operating inventory exhibits more impact scores than the BES components across all midpoint categories. The MEI of BES components, as expected, is negligible in comparison to the operating inventory. This result is consistent with those obtained by Sadhukhan (2017) and Foley et al. (2010), where the environmental impact of BES construction is minimal relative to its operational phase. Most interestingly, formic acid synthesis and COD removal *via* the BES show considerable environmental benefits across all midpoint impact categories. The presented environmental benefits are due to the displacement of fossil-based formic acid production and electricity required for equivalent COD removal in an activated sludge plant. The environmental impact of the equal mixes (average) fossil-based HCOOH is overwhelmingly more than the combined

Table 5b
Total operating cost components.

Cost component	Amount per yr	Value (€/yr)
Anolyte	2.54 m^3	0.0029
Catholyte	0.013 m^3	0.0069
Electricity input	0.024 kWh	0.0034
Maintenance cost	–	0.016
Total operating cost	–	0.029

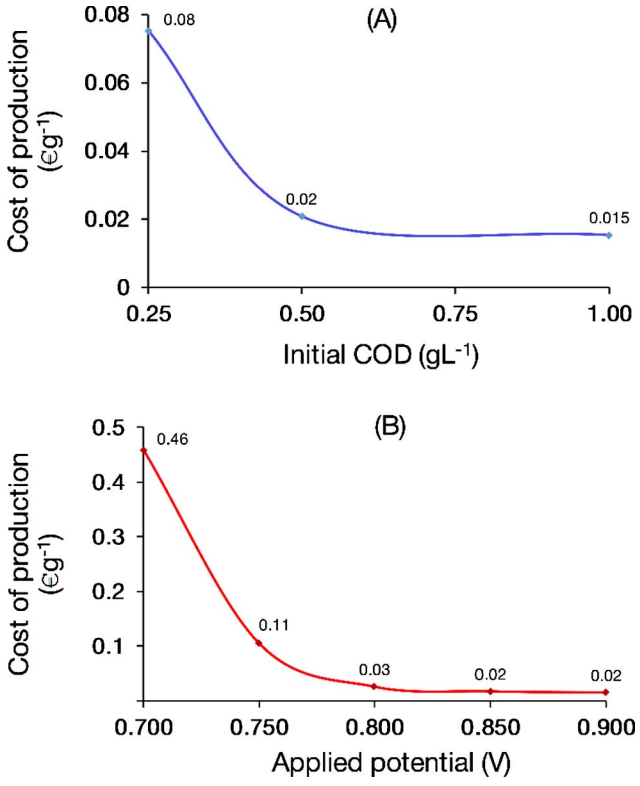

Fig. 5. A and B Effects of changes in initial COD (at constant applied potential of 0.9 V) and applied potential (at constant initial COD of 1 gL^{-1}) on the cost of production, respectively.

environmental impacts of the BES (i.e. components and operating inventory) across all midpoint categories, thus giving the highest environmental impact saving by the displacement of fossil-based production methods. Thus, as shown in Table 6, significant environmental burden can be avoided from the displacement of fossil-based production methods by BES-synthesised HCOOH. The avoided environmental burden from the displacement of fossil-based wastewater treatment methods by BES-treated water is less than that from the displacement of fossil-based production methods by BES-synthesised HCOOH. The avoided environmental burdens by each functionality of BES, formic acid synthesis and wastewater treatment, are shown without and with economic allocations between the two functionalities, price of formic acid and cost of COD removal by activated sludge process, with no difference in conclusions, apart from the quantities of the net MEI savings.

The endpoint impact potential costs due to BES operating and assemblage, and benefits due to avoided grid electricity for COD removal for wastewater treatment by activated sludge process and avoided global average fossil-based HCOOH production on climate change, resources, human health and ecosystem quality are depicted in Fig. 6.

The environmental impact costs of BES operating inventory (−5%) are noticeable than those exhibited by BES assemblage (~0%) in all endpoint categories; nevertheless, they are outweighed by the environmental benefits of HCOOH synthesis (93%) and COD removal (12%) by BES. The LCA results obtained in this study are comparable to that obtained by Sadhukhan (2017), e.g. in climate change potential saving: 2.5 kg CO_2-eq; resources saving potential: 61 MJ, and that shows the environmental benefits of avoided products sufficiently offset the environmental costs. While LCA shows strong drivers for BES with respect to all environmental impact categories, TEA shows the need for scale-up for commercial application of BES. It is foreseeable to the authors that BES will create opportunities in resource recovery and productivity from waste in the context of circular economy, due to its modular approach, which means a proven cost-effective and optimal module can be repeated to meet a given throughput; multi-functionality and a high range of product slate; and increasing number of competitive robust designs towards commercialisation.

4. Conclusions

An integrated framework for DS, TEA and LCA of BES has been demonstrated using HCOOH synthesis as a case study. Substrate concentration (initial COD) and applied potential have been found to have

Table 6
Midpoint impacts of BES operating (O), assemblage (A) and total; COD removal by activated sludge process (COD-R) and average fossil-based HCOOH production (FA-P), and net MEI saving analysis (basis: 1 kg HCOOH and thus, 0.406 kg COD removal). TEG: Triethylene glycol.

	BES (O)	BES (A)	Total BES	COD-R	FA-P	Net MEI savings			
						w/o allocation		w economic allocation	
Impact category						COD-R	FA-P	COD-R	FA-P
Carcinogens (kg C_2H_3Cl eq)	7.7×10^{-4}	7.9×10^{-7}	7.7×10^{-4}	8.2×10^{-4}	0.07	5.2×10^{-5}	6.9×10^{-2}	8.0×10^{-4}	6.9×10^{-2}
Non-carcinogens (kg C_2H_3Cl eq)	7.6×10^{-4}	2.6×10^{-6}	7.7×10^{-4}	1.6×10^{-3}	0.03	7.9×10^{-4}	2.6×10^{-2}	1.5×10^{-3}	2.6×10^{-2}
Respiratory inorganics (kg $PM_{2.5}$ eq)	1.4×10^{-4}	5.9×10^{-8}	1.4×10^{-4}	3.3×10^{-7}	2.3×10^{-3}	1.9×10^{-4}	2.2×10^{-3}	3.3×10^{-4}	2.2×10^{-3}
Ionizing radiation (Bq C-14 eq)	6.32	2.3×10^{-4}	6.32	18.97	32.15	12.65	25.83	18.84	25.97
Ozone layer depletion (kg CFC-11 eq)	9.5×10^{-9}	3.0×10^{-9}	1.2×10^{-8}	2.5×10^{-8}	3.7×10^{-7}	1.2×10^{-8}	3.6×10^{-7}	2.5×10^{-8}	3.6×10^{-7}
Respiratory organics (kg C_2H_4 eq)	1.2×10^{-5}	1.7×10^{-8}	1.2×10^{-5}	2.7×10^{-5}	1.6×10^{-3}	1.5×10^{-5}	1.6×10^{-3}	2.7×10^{-5}	1.6×10^{-3}
Aquatic ecotoxicity (kg TEG: triethylene glycol water)	6.76	0.02	6.78	17.61	154.61	10.82	147.84	17.46	147.98
Terrestrial ecotoxicity (kg TEG soil)	1.75	0.01	1.76	4.42	42.48	2.66	40.71	4.38	40.75
Terrestrial acidification (kg SO_2 eq)	2.3×10^{-3}	1.1×10^{-6}	2.3×10^{-3}	6.3×10^{-3}	0.04	4.0×10^{-3}	3.3×10^{-2}	6.2×10^{-3}	3.3×10^{-2}
Land occupation (m^2)	2.4×10^{-3}	7.1×10^{-7}	2.4×10^{-3}	6.1×10^{-3}	0.04	3.7×10^{-3}	3.9×10^{-2}	6.0×10^{-3}	3.9×10^{-2}
Aquatic acidification (kg SO_2 eq)	8.7×10^{-4}	2.8×10^{-7}	8.7×10^{-4}	2.4×10^{-3}	0.01	1.5×10^{-3}	1.1×10^{-2}	2.4×10^{-3}	1.1×10^{-2}
Aquatic eutrophication (kg Phosphate eq)	2.5×10^{-5}	2.0×10^{-7}	2.5×10^{-5}	5.9×10^{-5}	6.1×10^{-4}	3.4×10^{-5}	5.9×10^{-4}	5.8×10^{-5}	5.9×10^{-4}
Global warming (kg CO_2 eq)	0.17	6.7×10^{-5}	0.17	0.46	4.02	0.29	3.85	0.45	3.86
Non-renewable energy (MJ primary)	2.79	3.5×10^{-4}	2.79	7.86	55.65	5.07	52.86	7.80	52.92
Mineral extraction (MJ surplus)	2.6×10^{-3}	5.4×10^{-5}	2.7×10^{-3}	2.6×10^{-3}	0.11	-1.7×10^{-4}	1.1×10^{-1}	2.5×10^{-3}	1.1×10^{-1}

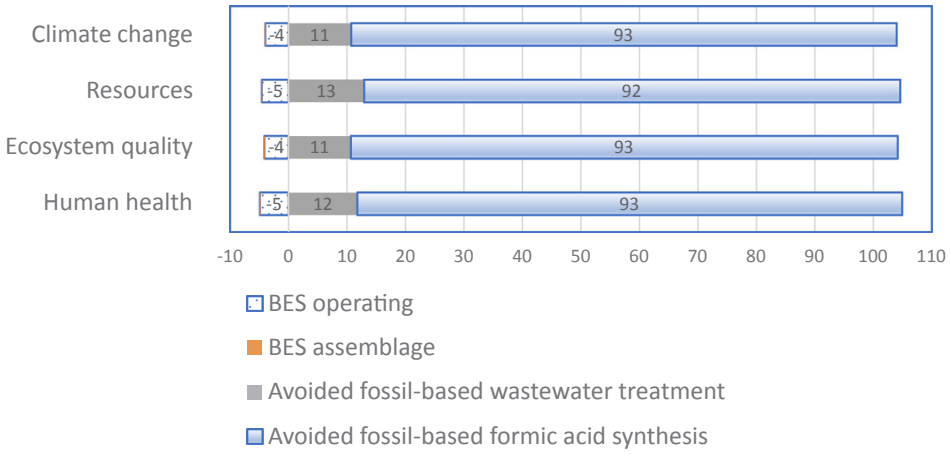

Fig. 6. Life cycle impact potential benefits (shown on + x axis) and costs (shown on -x axis) and thus net savings of BES in Impact 2002 + end point categories normalised to 100. The net saving amounts on the basis of 1 kg formic acid synthesis and thus 0.406 kg COD removal are in climate change: 4.3 kg CO_2-eq; resources: 61 MJ; ecosystem quality: 0.46 Potentially Disappeared Fraction (PDF) of species over a specific area (m^2) during on year; human health: 2.06×10^{-6} Disability-adjusted life years (DALY) describes the severity of disease, in terms of mortality and morbidity.

strongest influence on the rates of COD removal and HCOOH production, and consequently, the cost of production. DS correlations are used in TEA/LCA for holistic evaluation of BES. Membrane and maintenance costs are the major contributors to capital and operating costs, respectively. BES (assemblage and operational) shows significant environmental benefits in comparison to current fossil-based industrial methods for the provision of same functionalities, product synthesis and wastewater treatment.

Acknowledgements

The authors gratefully acknowledge the financial support provided for this work by the UK Engineering and Physical Sciences Research Council (EPSRC) project reference: EP/N009746/1 and the Natural Environment Research Council (NERC) project reference: NE/L014246/1.

References

Alvarez-Guerra, M., Del Castillo, A., Irabien, A., 2014. Continuous electrochemical reduction of carbon dioxide into formate using a tin cathode: Comparison with lead cathode. Chem. Eng. Res. Des. 92, 692–701. http://dx.doi.org/10.1016/J.CHERD.2013.11.00.

Bajracharya, S., Sharma, M., Mohanakrishna, G., Dominguez Benneton, X., Strik, D.P.B.T.B., Sarma, P.M., Pant, D., 2016. An overview on emerging bioelectrochemical systems (BESs): technology for sustainable electricity, waste remediation, resource recovery, chemical production and beyond. Energy Renew. http://dx.doi.org/10.1016/j.renene.2016.03.002.

Call, D., Logan, B., 2008. Hydrogen production in a single chamber microbial electrolysis cell lacking a membrane. Sci. Technol. Environ. http://dx.doi.org/10.1021/es8001822.

Chen, B.Y., Liu, S.Q., Hung, J.Y., Shiau, T.J., Wang, Y.M., 2013. Reduction of carbon dioxide emission by using microbial fuel cells during wastewater treatment. Aerosol Air Qual. Res. https://doi.org/10.4209/aaqr.2012.05.0122.

Christodoulou, X., Velasquez-Orta, S.B., 2016. Microbial electrosynthesis and anaerobic fermentation: an economic evaluation for acetic acid production from CO_2 and CO. Environ. Sci. Technol. http://dx.doi.org/10.1021/acs.est.6b02101.

Dang, Q., Wright, M.M., Li, W., 2017. Technoeconomic analysis of a hybrid biomass thermochemical and electrochemical conversion system. Energy Technol. http://dx.doi.org/10.1002/ente.201700395.

Ecoinvent, 2013. Ecoinvent Database 3.0. Ecoinvent Cent. doi:10.4018/978-1-59140-342-5.ch003.

Foley, J., Rozendal, R.A., Hertle, C.K., Lant, P.A., Rabaey, K., 2010. Life cycle assessment of high-rate anaerobic treatment, microbial fuel cells, and microbial electrolysis cells. Environ. Sci. Technol. 44, 3629–3637. http://dx.doi.org/10.1021/es100125h.

Guerrini, A., Romano, G., Indipendenza, A., 2017. Energy efficiency drivers in wastewater treatment plants: a double bootstrap DEA analysis. Sustain. 9, 1–13. http://dx.doi.org/10.3390/su9071126.

Hori, Y., Wakebe, H., Tsukamoto, T., Koga, O., 1994. Electrocatalytic process of CO selectivity in electrochemical reduction of CO_2 at metal electrodes in aqueous media. Acta Electrochim. http://dx.doi.org/10.1016/0013-4686(94)85172-7.

Humbert, S., Schryver, A. De, Bengoa, X., Margni, M., Jolliet, O., 2012. IMPACT 2002+: User Guide vQ2.21.

IHS Markit, 2017. Formic Acid - Chemical Economics Handbook (CEH) | IHS Markit URL https://www.ihs.com/products/formic-acid-chemical-economics-handbook.html (accessed 10.7.17).

IPCC, 2014. Summary for Policymakers, In: Climate Change 2014, Mitigation of Climate Change. Contribution of Working. Group III to the Fifth Assessment Report of the Intergovernmental Panel on Climate change. Cambridge University Press, Cambridge, United Kingdom, New York, NY, USA.

ISO 14044: Environmental management – Life cycle assessment – Requirements and guidelines. Int. Organ. Stand. doi:10.1136/bmj.332.7555.1418.

ISO 14040: Environmental management – Life Cycle Assessment – Principles and Framework. Int. Organ. Stand. doi:10.1016/j.ecolind.2011.01.007.

ISO 14041, 1998. Environmental management – life cycle assessment – goal and scope definition – inventory analysis. Int. Organ. Stand.

Kaewsuk, J., Thorasampan, W., Thanuttamavong, M., Seo, G.T., 2010. Kinetic development and evaluation of membrane sequencing batch reactor (MSBR) with mixed cultures photosynthetic bacteria for dairy wastewater treatment. J. Environ. Manage. https://doi.org/10.1016/j.jenvman.2010.01.012.

Karimi Alavijeh, M., Mardanpour, M.M., Yaghmaei, S., 2015. A generalized model for complex wastewater treatment with simultaneous bioenergy production using the microbial electrochemical cell. Acta Electrochim. http://dx.doi.org/10.1016/j.electacta.2015.03.133.

Kim, H.S., Morgan, R.D., Gurau, B., Masel, R.I., 2009. A miniature direct formic acid fuel cell battery. J. Power Sources 188, 118–121. http://dx.doi.org/10.1016/j.jpowsour.2008.11.082.

Köleli, F., Balun, D., 2004. Reduction of CO_2 under high pressure and high temperature on Pb-granule electrodes in a fixed-bed reactor in aqueous medium. Appl. Catal. A Gen. 274, 237–242. http://dx.doi.org/10.1016/J.APCATA.2004.07.006.

Marcus, A.K., Torres, C.I., Rittmann, B.E., 2007. Conduction-based modeling of the biofilm anode of a microbial fuel cell. Biotechnol. Bioeng. http://dx.doi.org/10.1002/bit.21533.

Ng, K.S., Head, I., Premier, G.C., Scott, K., Yu, E., Lloyd, J., Sadhukhan, J., 2016. A multilevel sustainability analysis of zinc recovery from wastes. Resourc. Conserv. Recycl. 113, 88–105. http://dx.doi.org/10.1016/j.resconrec.2016.05.013.

Pant, D., Singh, A., Van Bogaert, G., Gallego, Y.A., Diels, L., Vanbroekhoven, K., 2011. An introduction to the life cycle assessment (LCA) of bioelectrochemical systems (BES) for sustainable energy and product generation: Relevance and key aspects. Renew. Sustain. Energy Rev. 15, 1305–1313. http://dx.doi.org/10.1016/j.rser.2010.10.005.

Pant, D., Van Bogaert, G., Diels, L., Vanbroekhoven, K., 2010. A review of the substrates used in microbial fuel cells (MFCs) for sustainable energy production. Bioresour. Technol. 101, 1533–1543. http://dx.doi.org/10.1016/j.biortech.2009.10.017.

Pérez-Fortes, M., Schöneberger, J.C., Boulamanti, A., Harrison, G., Tzimas, E., 2016. Formic acid synthesis using CO_2 as raw material: techno-economic and environmental evaluation and market potential. Int. J. Hydrogen Energy 41, 16444–16462. http://dx.doi.org/10.1016/j.ijhydene.2016.05.199.

Pinto, R.P., Srinivasan, B., Escapa, A., Tartakovsky, B., 2011. Multi-population model of a microbial electrolysis cell. Sci. Technol. Environ. http://dx.doi.org/10.1021/es104268g.

Puyol, D., Batstone, D.J., Hülsen, T., Astals, S., Peces, M., Krömer, J.O., 2017. Resource recovery from wastewater by biological technologies: Opportunities, challenges, and prospects. Microbiol Front. http://dx.doi.org/10.3389/fmicb.2016.02106.

Rabaey, K., Angenent, L., Schröder, U., Keller, J., 2009. Bioelectrochemical systems : from extracellular electron transfer to biotechnological application. IWA publishing.

Rabaey, K., Rozendal, R.A., 2010. Microbial electrosynthesis – revisiting the electrical route for microbial production. Nat. Rev. Microbiol. 8, 706–716 10.1038/nrmicro2422.

Rice, C., Ha, S., Masel, R.I., Waszczuk, P., Wieckowski, A., Barnard, T., 2002. Direct formic acid fuel cells. J. Power Sources 111, 83–89 10.1016/S0378-7753(02)00271-9.

Rosso, D., Stenstrom, M.K., 2008. The carbon-sequestration potential of municipal wastewater treatment. Chemosphere 10.1016/j.chemosphere.2007.08.057.

Rozendal, A., Hamelers, H.V.M., Rabaey, K., Keller, J., Buisman, C.J.N., 2008. Towards practical implementation of bioelectrochemical wastewater treatment. Trends Biotechnol. http://dx.doi.org/10.1016/j.tibtech.2008.04.008.

Sadhukhan, J., Martinez-Hernandez, E., Murphy, R.J., Ng, D.K., Hassim, M.H., Ng, K.S., Kin, W.Y., Jaye, I.F.M., Hang, M.Y.L.P., Andiappan, V., 2018. Role of bioenergy,

biorefinery and bioeconomy in sustainable development: Strategic pathways for Malaysia. Ren. Sus. Energy Rev. 81, 1966–1987. http://dx.doi.org/10.1016/j.rser.2017.06.007.

Sadhukhan, J., Joshi, N., Shemfe, M., Lloyd, J.R., 2017. Life cycle assessment of sustainable raw material acquisition for functional magnetite bionanoparticle production. J. Environ. Manage. 199, 116–125. http://dx.doi.org/10.1016/j.jenvman.2017.05.048.

Sadhukhan, J., 2017. Microbial electrosynthesis. In: Encyclopedia of Sustainable Technologies. Elsevier, pp. 455–468.

Sadhukhan, J., Lloyd, J.R., Scott, K., Premier, G.C., Yu, E.H., Curtis, T., Head, I.M., 2016. A critical review of integration analysis of microbial electrosynthesis (MES) systems with waste biorefineries for the production of biofuel and chemical from reuse of CO_2. Renew. Sustain. Energy Rev. 56, 116–132. http://dx.doi.org/10.1016/j.rser.2015.11.015.

Sadhukhan, J., Ng, K.S., Hernandez, E.M., 2014. Biorefineries and chemical processes: design integration and sustainability analysis. Wiley Blackwell.

Shemfe, M., Sadhukhan, J., Ng, K.S., 2018. Bioelectrochemical Systems for biofuel (electricity, hydrogen, and methane) and valuable chemical production. In: Gnaneswar, V. (Ed.), Green Chemistry for Sustainable Biofuel Production. Apple Academic Press.

Wang, Q., Dong, H., Yu, H., Yu, H., Liu, M., 2015. Enhanced electrochemical reduction of carbon dioxide to formic acid using a two-layer gas diffusion electrode in a microbial electrolysis cell. RSC Adv. http://dx.doi.org/10.1039/C4RA14535F.

Xu, S., Luo, L., Selvam, A., Wong, J.W.C., 2017. 6 – Strategies to increase energy recovery from phase-separated anaerobic digestion of organic solid waste. Dev. Biotechnol. Bioeng. Curr. http://dx.doi.org/10.1016/B978-0-444-63664-5.00006-X.

Zhao, H.Z., Zhang, Y., Chang, Y.Y., Li, Z.S., 2012a. Conversion of a substrate carbon source to formic acid for carbon dioxide emission reduction utilizing series-stacked microbial fuel cells. J. Power Sources. http://dx.doi.org/10.1016/j.jpowsour.2012.06.014.

Zhao, H., Zhang, Y., Zhao, B., Chang, Y., Li, Z., 2012b. Electrochemical reduction of carbon dioxide in an MFC-MEC system with a layer-by-layer self-assembly carbon nanotube/cobalt phthalocyanine modified electrode. Sci. Technol. Environ. http://dx.doi.org/10.1021/es300186f.